Abdominal Imaging


Published online: 5 May 2007

Abdom Imaging (2008) 33:313–323
DOI: 10.1007/s00261-007-9244-y

# Double-contrast magnetic resonance imaging of hepatocellular carcinoma after transarterial chemoembolization

Nicolae Bolog,[1] Thomas Pfammatter,[1] Beat Müllhaupt,[2] Gustav Andreisek,[1] Dominik Weishaupt[1]

[1]Department of Magnetic Resonance, Institute of Diagnostic Radiology, Zurich, Switzerland
[2]Department of Gastroenterology, University Hospital, Zurich, Switzerland

## Abstract

*Background:* The purpose of this study was to assess the accuracy of double-contrast magnetic resonance (MR) imaging for the treatment response evaluation of hepatocellular carcinoma (HCC) in cirrhotic liver after transarterial chemoembolization (TACE).
*Methods:* Twenty-two patients with 30 HCC nodules treated by TACE underwent double-contrast MR imaging 1 month after treatment. MR images were obtained before and after the sequential administration of superparamagnetic iron oxide (SPIO) and gadopentetate dimeglumine contrast agent within the same imaging session. Two observers retrospectively assessed all treated nodules for evidence of residual viable tumor after TACE. The diagnostic performance of gadolinium-enhanced, SPIO-enhanced, and double-contrast enhanced images was calculated. Histopathological and angiographical findings served as standard of reference. Receiver operating characteristic curves and areas under the curves ($A_z$) were calculated.
*Results:* Double-contrast technique ($A_z$ = 0.95) was significantly ($p$ = 0.036) more accurate than SPIO-enhanced technique ($A_z$ = 0.92) and gadolinium-enhanced technique ($p$ = 0.005) ($A_z$ = 0.81) in viable tumor detection after TACE. Double-contrast technique was significantly more sensitive (92%) than SPIO-enhanced technique (80%) and gadolinium-enhanced technique (68%). Kappa values for interobserver agreement ranged from 0.67 to 0.87 and were significantly different from zero (all $p < 0.001$).
*Conclusions:* Compared to gadolinium-enhanced and SPIO-enhanced techniques, double-contrast technique significantly improves the detection of viable tumor in HCC after TACE.

Cirrhosis—Superparamagnetic iron oxide (SPIO)—Transarterialchemoembolization (TACE)—Hepatocellular carcinoma (HCC)—Double-contrast MR imaging

Hepatocellular carcinoma (HCC) is the most common primary liver malignant tumor. Although, either liver transplantation or surgical resection is the best curative option for HCC, these treatments are offered to a limited patient population because of the lack of hepatic reserve or because of the high rate of HCC progression while the patients are on the transplantation list [1].

Transarterial chemoembolization (TACE) is widely used in the treatment of patients who will not benefit from curative approaches or as a bridge to liver transplant. According to Barcelona-Clinic Liver Cancer group (BCLC) patients with early stages (i.e., one or a maximum of three HCC nodules < 3 cm) and good liver function should undergo tumor resection, transplantation or percutaneous treatment (i.e., percutaneuos ethanol injection or thermoablation) [2]. Child-Pugh A or B patients beyond these tumor stages may benefit from chemoembolization.

Most centers perform computed tomography (CT) (unenhanced and dynamic-enhanced) for TACE response evaluation. The most frequently used evaluation criteria is tumor necrosis defined as the absence of nodule enhancement on contrast-enhanced studies and the

*Correspondence to:* Dominik Weishaupt; *email:* dominik.weishaupt@usz.ch

amount of iodized oil emulsion storage on unenhanced scans. However, the nodules which were treated by TACE display areas of high attenuation on unenhanced CT images due to the iodized oil deposition, which results in difficulties with regard to the analysis of the enhancement pattern of the nodules following contrast administration. Moreover, tumor necrosis defined by the extension of iodized oil emulsion is probably not a good parameter since it has been shown that iodized oil retention does not always indicate necrosis [3].

Double-contrast MR imaging consists on the administration of superparamagnetic iron oxide (SPIO) and gadopentetate dimeglumine contrast agents in the same imaging session. By combining the enhancement pattern of the nodules after gadolinium administration on one hand and the tissue-specific information obtained after SPIO administration on the other, this technique has been demonstrated to improve the detection of HCC nodules in cirrhotic livers [4]. We hypothesized that the double-contrast MR technique would improve the detection of viable tumor after TACE and a retrospective multiobserver analysis involving our patients treated by TACE was performed.

The main objective of this study was to assess the accuracy of double-contrast magnetic resonance (MR) technique performed one month after TACE for the treatment response evaluation of HCC in cirrhotic liver. The secondary objective of this study was to describe the signal intensities of nodules with versus without viable tumor on unenhanced, SPIO-enhanced, and Gd-enhanced images.

## Materials and methods

### *Patients*

Between July 2001 and June 2004, 65 patients with HCC underwent TACE at our institution. Of these patients we included in our study only those patients who fulfilled the following criteria: first, the patients underwent double-contrast MR imaging one month after TACE without any intervention in the meantime; and second, histological or angiographical findings were available as standard of reference. Forty-three patients did not fulfill these criteria: 26 patients underwent double-contrast MR imaging later than one month after TACE, 11 patients had not undergone double-contrast MR imaging after TACE, and in six patients there were no angiographical or histological findings as standard of references. Twenty-two patients (16 men, 6 women, mean age 57.8 years, age range 24–74 years) fulfilled these criteria. Fourteen patients had undergone one TACE session, seven had undergone two, and one had undergone four chemoembolization sessions. All patients had biopsy-proved liver cirrhosis: posthepatitis C in nine patients, posthepatitis B in five patients, alcohol-induced cirrhosis in six patients, and mixed etiology in two patients. Among the 22 patients, TACE was performed in 30 HCC nodules and these nodules were the focus of this study. Seventeen patients had one nodule, three patients had two nodules, one patient had three nodules, and another patient had four chemoembolized nodules. Three patients with one nodule were treated in two sessions of segmental chemoembolization. In all patients with two nodules chemoembolization was carried out separately for each nodule by segmental injection of iodized oil emulsion. The patient with three nodules underwent two different sessions of treatment which consisted of one segmental embolization for one nodule and one lobar embolization for two nodules. The patient with four nodules underwent four different sessions represented by three segmental chemoembolizations for one nodule and one lobar chemoembolization for three nodules. Double-contrast MR images were obtained 27–30 days (mean 28 days) after each session of segmental or lobar TACE in 18 patients (14 patients with one nodule, one patient with three nodules, and three patients with two nodules). In the three patients with one nodule who underwent two sessions of treatment the MR images were obtained 27–29 days after the second chemoembolization. In the patient with four nodules the MR images were obtained 30 days after the third TACE for one nodule and 29 days after lobar TACE for the remaining three nodules. The long axis diameter of the nodules ranged from 12 to 74 mm (mean 31.1 mm) as measured on T1-unenhanced images.

Our institutional review board does not require patient approval or informed consent for reviewing patient images. Patient rights are protected by a law that requires patients to be informed at examination time about the possibility that their images might be used for scientific purposes.

### *MR imaging*

All images were obtained using a 1.5-T scanner (Signa Echospeed or Excite HD, GE Healthcare, Waukesha). The imaging protocol included a transaxial respiratory-triggered T2-unenhanced fast spin-echo (FSE) sequence [repetition time (TR)/echo time (TE) = 3500–5714/99–106 ms; echo-train length (ETL) 12; 2 NEX; field-of-view (FOV) 32–35 × 22–24 cm; matrix, 256 × 256; section thickness, 6–8.0 mm; intersection gap, 2.0 mm] and transaxial T1-unenhanced fast spoiled gradient-recalled echo (FSPGR) sequences in- and out-of-phase during suspended respiration (TR/TE = 150–200/4.2–4.4 ms for in-phase acquisition and TR/TE = 120–180/1.5–2.2 ms for out-of-phase acquisition; flip angle, 60°; 1 NEX; FOV, 32–35 × 22–24 cm; matrix, 256 × 192 section thickness, 6.0–8.0 mm without spacing).

After obtaining the unenhanced sequences, 1.4 ml of SPIO ferucarbotran (Resovist®, Schering AG, Berlin, Germany) was administered in all patients as an i.v.

bolus (corresponding to 0.7 mmol Fe) followed by 20 ml saline flush. After 15–20 min, transaxial T2-weighted FSE sequences were performed with the same parameters as described above for T2-unenhanced images. The patients remained in the scanner throughout the examination. However, it was decided to perform the post-contrast examination with parameter settings optimized during a prescan performed after contrast-administration to account for the changes in signal intensity and to attempt to produce best image quality in each scan. Finally, a transaxial dynamic frequency-selective fat saturated T1-weighted two-dimensional FSPGR MR sequence in arterial, portal-venous and extracellular phase was performed (TR/TE = 150–170/1.4 ms; flip angle, 60°; 1 NEX; FOV, 32–35 × 22–24 cm; matrix, 256 × 192; section thickness, 6.0–8.0 mm without spacing). The delay between Resovist® administration and dynamic T1-weighted MR sequence was between 23 and 28 min. Gadopentetate dimeglumine was administered as an i.v. bolus at a dose of 0.2 ml/kg bodyweight (0.1 mmol/kg bodyweight) with a flow rate of 2 ml/s followed by a 20-ml saline flush at the same flow rate using a power injector (Spectris®, Medrad, Indianola, PA, USA). The injection time ranged between 6–10 s. The dynamic T1-weighted sequences were obtained with the same parameters as described above for the T1-unenhanced sequences. To ensure proper acquisition of the hepatic arterial phase images, bolus timing was performed using 1 ml of gadopentetate dimeglumine. Abdominal aorta was scanned once per second using a single slice transaxial FSPGR sequence repeatedly acquired to observe the wash-in of the gadopentetate dimeglumine contrast agent into the abdominal aorta [5]. The mean scanning delay of the arterial phase was approximately 18 s (range 14–29 s). Portal-venous phase and extracellular phase imaging were performed 60 and 180 s, respectively, after injection of the contrast medium.

## *TACE protocol*

The decision of performing TACE was based on clinical and imaging criteria and TACE was performed in patients who were not suitable for surgical treatment or patients who were waiting for liver transplant. The diagnosis of HCC was histological proved in 20 nodules. In ten nodules the diagnosis was based on correlation between imaging findings (MR imaging and DSA) and clinical data, including the alpha-fetoprotein level. Child C disease, tumor thrombus in the main left or right portal trunk, or extrahepatic metastasis was considered contraindication for chemoembolization. TACE was performed with a digital angiography unit (Integris 5000; Philips, Eindhoven, The Netherlands). Standard angiography was obtained with a 5F-curved endhole catheter introduced in the proper hepatic artery if no anatomic variant was present. If not, the replaced hepatic arteries were selected. Embolization was carried out by segmental or lobar injection of iodized oil emulsion (Lipiodol; 5–10 mL, Guerbet, Aulnay-sous-Bois, France) and doxorubicin hydrochloride (Adribastin, 40–50 mg, Pfizer, Switzerland) followed by PVA particles (250–350 μm). After embolization, an angiographic study of the liver was performed to confirm tumor devascularization. TACE procedures were performed by a single radiologist.

## *Image analysis*

Image analysis was performed on a dedicated workstation (Advantage Windows 4.1; GE Healthcare, Waukesha, WI, USA). Two experienced radiologists in abdominal imaging (reader 1 with 10 years of experience and reader 2 with 5 years of experience) separately assessed all imaging data. Both observers were blinded to clinical data but were informed about location of treated nodules (by giving the number of the corresponding Couinaud's liver segments). Regarding those patients with more than one nodule in the same segment, the readers were asked to differentiate the nodules based on the long axis diameter. The smallest nodule within the segment was considered the first-assessed nodule. Patients were randomized and three sets of images were presented at reading sessions in different order for each reader: the unenhanced and gadolinium-enhanced images (gadolinium technique); the unenhanced and SPIO-enhanced images (SPIO technique), and the unenhanced, SPIO-enhanced and gadolinium-enhanced images (double-contrast technique). There was a two-week interval between each reading session.

### Signal intensity and enhancement patterns

Each nodule was assessed regarding the signal intensity and enhancement features. The signal intensity was first assessed on T1-unenhanced in-phase and T2-unenhanced FSE images relative to surrounding parenchyma as follows: hypointense, isointense, and hyperintense (homogeneous or inhomogeneous). On gadolinium technique the nodules were assessed as nodules with or without hypervascular areas. A hypervascular area was defined as a lesion that displayed a visibly early enhancement on arterial phase images (greater than that of adjacent parenchyma or greater than that of nodule on precontrast images) followed by a wash-out during later phases. On SPIO technique both readers were asked to match the signal intensity of the treated HCC relative to surrounding liver parenchyma on T2-weighted images before and after SPIO administration to one of the following patterns: isointense nodules and hyperintense nodules on T2-unenhanced images in which the signal intensity decreases after SPIO administration; nodules homogeneous hypointense before as well as after SPIO

administration; hypointense nodules relative to liver on T2-unenhanced images which displayed areas of hyperintensity on T2-weighted images after SPIO administration; and finally, isointense or hyperintense nodules on T2-unenhanced images which did not show a reduction in signal intensity on T2-weighted images after SPIO administration. In this analysis of the T2-characteristics on unenhanced and SPIO-enhanced T2-weighted FSE images we included only those hyperintense lesions whose T2-signal was different from cerebral spinal fluid since it is known that hyperintense signal similar to CSF in treated nodules may correspond to liquefied necrosis [6].

#### Diagnostic performance

A final assessment was made by both readers regarding the residual tumor presence or absence by using the criteria showed in Table 1 on each technique separately. For each assessment a 5-point confidence scale was assigned: 1-definitely no viable tumor; 2-probably no viable tumor; 3-indeterminate; 4-probably viable tumor; 5-definitely viable tumor.

### *Standard of reference*

Confirmation of the presence or absence of viable tumor was established by histological findings (transplantation, autopsy or tumor resection), or by DSA findings. The pathologist was notified of location of all nodules that had undergone double-contrast MR imaging after TACE and the gross specimens were reviewed by one radiologist together with the pathologist. DSA was performed in those cases with suspicion of viable HCC after TACE based on serum alpha-fetoprotein level or double-contrast MR images. DSA was considered an effective method for nodule evaluation since the presence of hypervascularized areas indicates residual HCC [6, 7]. The intervals between double-contrast MR examination and standard of references were as follows: 46–431 days for transplantations (mean 117.40 days); 91 and 202 days for autopsies; 50 days for tumor resection; and 20–340 days (mean 122.87 days) for angiographies.

### *Statistical analysis*

Descriptive results for assessment of signal intensity and enhancement pattern for each observer are reported in absolute and relative numbers. Interobserver agreement was assessed using Cohen's kappa, and kappa values were tested for significant difference than zero [8]. A $k$ value of 0 indicates poor agreement, a value of 0.01–0.20 indicates slight agreement, a value of 0.21–0.40 indicated fair agreement, a value of 0.41–0.60 indicated moderate agreement, a value of 0.61–0.80 indicated substantial agreement, and a value of 0.81–1.00 indicated an almost perfect agreement [8]. Sensitivity, specificity, and accuracy for viable tumor detection were calculated for each reader and each MRI technique. The statistical significance of any difference between gadolinium-enhanced, SPIO-enhanced and double-contrast enhanced techniques was assessed using the Wilcoxon and Student $t$ test. For each technique (gadolinium, SPIO, and double-contrast technique) binomial receiver operating characteristic (ROC) curves were calculated. The area under the ROC curve ($A_z$) was used to indicate the overall performance of each imaging techniques. Sensitivity, specificity and accuracy of the imaging criteria for the presence of viable tumor with each MR technique were assessed for only those nodules that were assigned a confidence rating of 1 or 2 versus 4 or 5. All statistics were calculated using the SPSS Software (SPSS Inc., Chicago, IL, USA).

## Results

### *Standard of reference*

A viable tumor was found in 26 of 30 nodules (87%). The standard of reference in these cases consisted of histopathological analysis (following transplantation-12 nodules, and autopsy-2 nodules), and DSA findings in 12 nodules. In four nodules (13%) no viable tumor was found at histopathological analysis.

### *Signal intensity and enhancement patterns*

Absolute and relative numbers for signal intensity and enhancement pattern assessment for each observer, as well as kappa values for the interobserver agreement are reported in Table 2. Kappa values for interobserver agreement ranged from 0.67 to 0.87 and were significantly different from zero (all $p < 0.001$).

#### Enhancement pattern on gadolinium-enhanced images

All nodules (15 from 30) that were assessed as hypervascular by both readers were nodules with viable tumor at standard of reference (DSA in five nodules and histological findings in ten nodules) (Fig. 1). Among the nodules assessed as nodules without hypervascular areas (ten for both readers) there were seven false negatives results. The standard of reference was DSA in three nodules and histological findings in seven nodules. In all these cases the nodules displayed an inhomogeneous hyperintense signal on T1-unenhanced images (Fig. 2). Both readers considered five nodules as indeterminate regarding the arterial enhancement. Four nodules were with viable tumor at standard of reference. In all these four nodules the standard of reference was DSA.

**Table 1.** Criteria for the presence or absence of viable HCC after TACE with each MR technique

| MR technique | Nodules with residual viable tumor | Nodules without residual viable tumor |
|---|---|---|
| Gadolinium-enhanced | Nodules with hypervascular areas[a] | Nodules without hypervascular areas |
| SPIO-enhanced | Nodules homogeneous hypointense on unenhaced T2-weighted images which display hyperintense areas on T2-weighted images after SPIO administration[b] | Nodules homogeneous hypointense on T2-weighted images before and after SPIO administration[c] |
| | OR | OR |
| | Nodules hyperintense or isointense on unenhanced T2-weighted images with no signal reduction after SPIO administration[b] | Nodules hyperintense or isointense on unenhanced T2-weighted images which decrease in signal after SPIO administration[d] |
| Double-contrast enhanced | Nodules assessed as nodules with viable tumor on gadolinium-enhanced images OR on SPIO-enhanced images | Nodules assessed as nodules without viable tumor on gadolinium-enhanced images AND on SPIO-enhanced images |

[a]Areas with a rapid enhancement on arterial phase images (greater than that of adjacent parenchyma or greater than that of nodule on precontrast images) followed by a wash-out during later phases on gadolinium-enhanced technique
[b]Areas without SPIO uptake which is considered as an indicator of malignancy (4)
[c]Nodules with coagulative necrosis (32)
[d]Areas with SPIO uptake which is considered as an indicator of the viable tumor absence (4)

**Table 2.** Signal intensity and enhancement pattern assessment of HCC treated with TACE

| MR images | Pattern | R1 no (%) | R2 no (%) | *k*-value (95% CI) | *P*-value | Nodules with viable tumor at SOR |
|---|---|---|---|---|---|---|
| Unenhanced T1 | Total | 30 (100%) | 30 (100%) | 0.87 (0.70–1) | < 0.001 | |
| | Hyperintense | 17 (57%) | 17 (57%) | | | 15 |
| | Hypointense | 2 (7%) | 2 (7%) | | | 1 |
| | Isointense | 11 (36%) | 11 (36%) | | | 10 |
| Unenhanced T2 | Total | 30 (100%) | 30 (100%) | 0.67 (0.44–0.90) | < 0.001 | |
| | Hyperintense | 16 (54%) | 16 (54%) | | | 14 |
| | Hypointense | 7 (23%) | 7 (23%) | | | 6 |
| | Isointense | 7 (23%) | 7 (23%) | | | 6 |
| Gadolinium-enhanced technique | Total | 30 (100%) | 30 (100%) | 0.67 (0.44–0.90) | < 0.001 | |
| | Hypervascular[a] | 15 (50%) | 15 (50%) | | | 15 |
| | Without hypervascular areas | 10 (34%) | 10 (34%) | | | 7 |
| | Indeterminate | 5 (16%) | 5 (16%) | | | 4 |
| SPIO-enhanced technique | Total | 30 (100%) | 30 (100%) | 0.75 (0.54–0.95) | < 0.001 | |
| | Nodules homogeneous isointense or hypointense on T2-unenhaced images which displayed hyperintense areas on T2-weighted images after SPIO administration[b] | 2 (7%) | 4 (13%) | | | 4 |
| | Nodules isointense or nodules with hyperintense areas on T2-unenhanced images with no signal reduction after SPIO administration[b] | 16 (53%) | 16 (53%) | | | 16 |
| | Nodules homogeneous hypointense before and after SPIO administration[c] | 6 (20%) | 5 (17%) | | | 1 |
| | Nodules isointense or with hyperintense areas on T2-unenhanced images which decrease in signal after SPIO administration[d] | 3 (10%) | 3 (10%) | | | 2 |
| | Indeterminate | 3 (10%) | 2 (7%) | | | 3 |

R1, reader 1; R2, reader 2; SOR, standard of reference
[a]Areas with a rapid enhancement on arterial phase images (greater than that of adjacent parenchyma or greater than that of nodule on precontrast images) followed by a wash-out during later phases on gadolinium-enhanced technique
[b]Areas without SPIO uptake which is considered as an indicator of malignancy (4)
[c]Nodules with coagulative necrosis (32)
[d]Areas with SPIO uptake which is considered as an indicator of the viable tumor absence (4)

### Signal intensity pattern on SPIO-enhanced images

All nodules (18 for reader one and 20 for reader 2) that displayed hyperintense areas with no reduction in signal intensity on T2-weighted images after SPIO administration were with residual viable tumor (Fig. 3). DSA was the standard of reference in nine nodules. This criterion was especially useful in the cases of the false negative results on gadolinium-enhanced technique (e.g., hyperintense nodules on T1-unenhanced

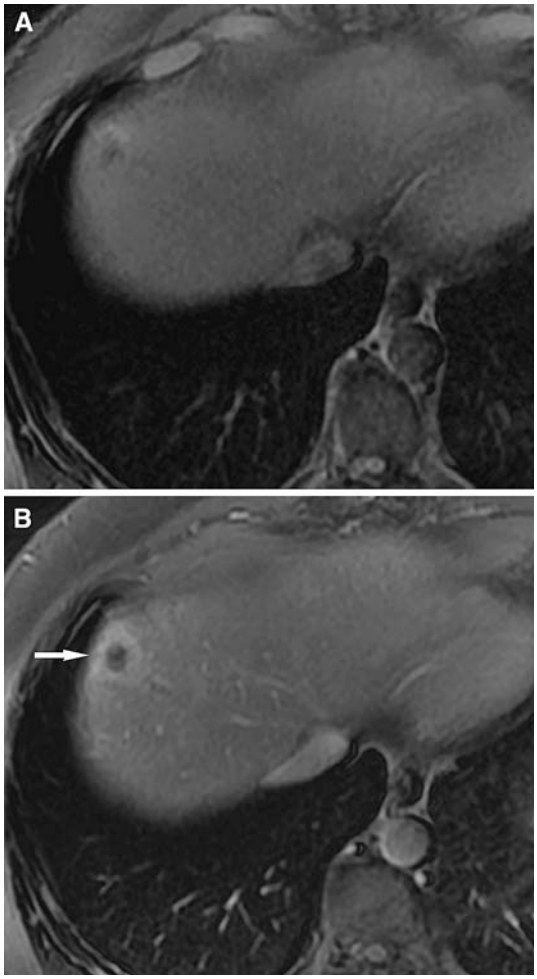


**Fig. 1.** Follow-up MR images of a 60-year-old male with HCC and liver cirrhosis obtained 29 days following TACE. **A** Transverse T1-weighted gradient-echo recalled MR image (210/1.3) before the administration of contrast agents shows a hypointense nodule. **B** Corresponding T1-weighted 2D FSPGR MR image (150/1.4) obtained 20 s after gadopentetate dimeglumine administration demonstrates a marked arterial enhancement of the periphery of the nodule indicating viable tumor (*arrow*). The nodule was considered a nodule with residual viable tumor and the result was confirmed at histopathology.

images) (Fig. 2). The homogeneous hypointense nodules before and after SPIO administration (6 for reader 1 and 5 for reader 2) were without viable tumor in four cases (Fig. 4). All nodules which were assessed as nodules with signal drop after SPIO administration were nodules with viable tumor at standard of reference (DSA in one nodule and histological findings in two nodules). Those nodules in which the readers were not confident in assigning an established pattern (indeterminate nodules) were nodules with viable tumor. DSA was the standard of reference in two nodules.

### *Diagnostic performance*

Sensitivities, specificities and accuracies for viable tumor detection for each observer and each MRI technique are shown in Table 3. For both readers, double-contrast technique was more accurate than SPIO-enhanced and gadolinium-enhanced techniques. There was a significant difference between double-contrast and SPIO-enhanced technique (R1, $p = 0.032$; R2, $p = 0.009$) and between double-contrast and gadolinium-enhanced technique (R1, $p = 0.009$; R2, $p = 0.003$). No significant differences were found between gadolinium-enhanced and SPIO-enhanced technique (R1, $p = 0.454$; R2, $p = 0.126$). ROC curves for viable tumor detection are shown in Fig. 5. Corresponding $A_z$ values for gadolinium-enhanced technique were 0.81, for SPIO-enhanced technique 0.92, and for double-contrast technique 0.95. Overall performance for double-contrast technique was significantly higher than gadolinium-enhanced ($p = 0.005$) and SPIO-enhanced technique ($p = 0.036$) regarding detection of viable tumor. No significant difference for the overall performance of viable tumor detection was found between gadolinium and SPIO-enhanced techniques ($p = 0.28$).

## Discussion

Complete necrosis of HCC is rarely accomplished with TACE. Therefore different imaging modalities for evaluation of TACE efficacy have been described. Many studies [9–12] have shown that the TACE effectiveness can be judged based on the degree of iodized oil retention, as a close correlation between accumulation of iodized oil emulsion and tumor necrosis has been demonstrated histologically [13, 14]. A complete retention of iodized oil emulsion on CT images was correlated with a 98% necrosis of resected specimen [11]. Imaeda et al. [9] evaluated the effectiveness of TACE based on the measurements of attenuation values of the nodules after TACE. These authors concluded that a cutoff value of 365 HU corresponded to massive necrosis (> 97% of the nodule) with 89% sensitivity and 73% specificity. A more accurate evaluation of necrotic areas was obtained by combining unenhanced CT with contrast-enhanced CT [15, 16]. The necrotic areas were defined as iodized oil retention areas and areas with no enhancement on contrast-enhanced CT. By using these criteria, Okusaka et al. [16], demonstrated a significant correlation between tumor necrosis at CT and tumor necrosis rate at histopathology.

Other authors [17–19] evaluated these two criteria as prognostic markers after TACE. In these studies, a homogeneous accumulation of iodized oil emulsion within the tumor on unenhanced-CT images was correlated with a high survival rate [17], while an incomplete iodized oil emulsion retention was followed by a higher rate of recurrence 1 year after treatment [18].

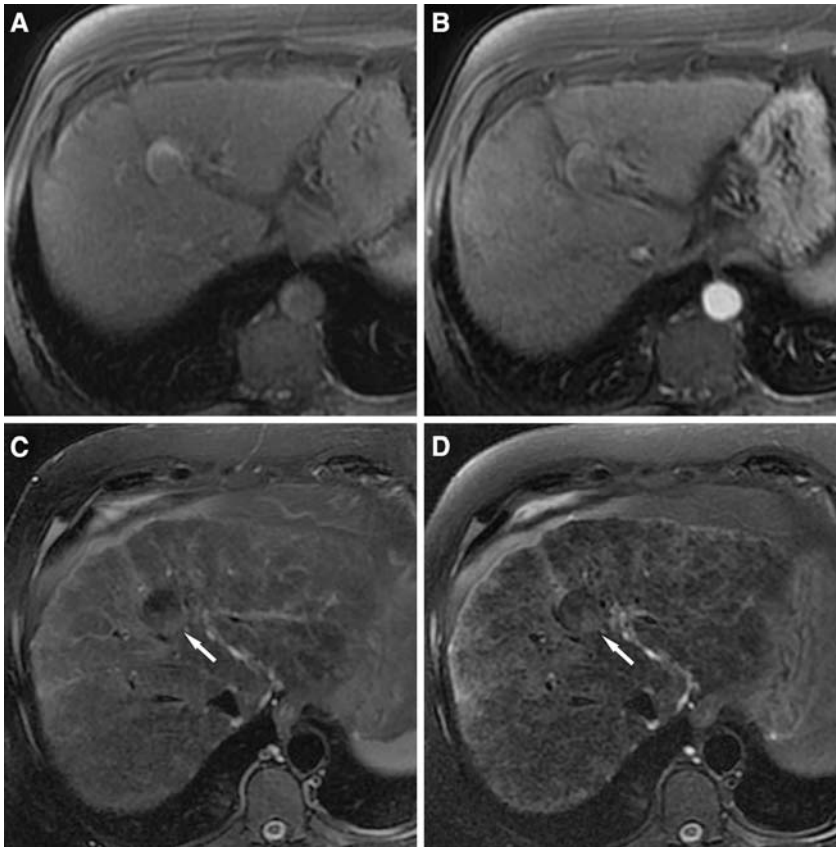


**Fig. 2.** Cirrhotic liver in a 58-year-old male with an HCC nodule in liver segment 4, 27 days after the first TACE. **A** Unenhanced transverse T1-weighted 2D GRE MR image (210/1.2) demonstrates an inhomogeneous hyperintense nodule compared to the liver parenchyma. **B** Transverse T1-weighted 2D FSPGR MR image (170/1.4) obtained 20 s after gadopentetate dimeglumine administration. Areas of early arterial enhancement cannot be discriminated within nodule which appears inhomogeneous hyperintense on either unenhanced and enhanced images. **C** Transverse respiratory-triggered T2-weighted FSE (5000/99.4 with fat suppression) at the same level before SPIO administration. The nodule is hypointense because of coagulative necrosis with a small hyperintense area at the periphery (*arrow*). **D** Transverse respiratory-triggered T2-weighted FSE (5000/99.4 with fat suppression) at the same level, 15 min after SPIO administration. Note the hyperintense area with no evidence of SPIO uptake which becomes more conspicuous at the periphery of the low signal intensity nodule (*arrow*). Based on this pattern, on double-contrast images, the nodule was correctly assessed as a nodule with viable HCC after TACE.

However, there is some evidence that assessment of tumor necrosis is probably not a good parameter for TACE evaluation since the tumor progression was noted even in nodules completely filled with iodized oil on unenhanced-CT [17, 20]. Moreover, Castrucci et al. [6] have demonstrated that the iodized oil absence in areas within the nodule does not always correspond to residual tumor. The patients who underwent TACE may develop local chemotherapy-induced vasculitis and vascular occlusions. Therefore, the non-enhancing areas on dynamic CT images may represent tumor, necrosis or fibrosis [21].

In addition to these CT studies there are several studies with other imaging modalities (ultrasonography or dynamic contrast-enhanced MR using gadolinium-compounds) focusing on the residual tumor detection after TACE [3, 22–25]. Regardless the imaging technique, the diagnosis of viable HCC after TACE is mainly based on tumor vascularity, and is defined as an early arterial enhancing area. Koito et al. [22], using biopsy as standard of reference, reported a 66.6% sensitivity, a 100% specificity, and 93.6% accuracy for assessing tumor viability with power Doppler sonography. Doppler sonography can reveal tumor vascularity independently of iodized oil emulsion accumulation having an advantage over CT [26]. By using the microbubble contrast agents, ultrasonography enabled assessment of TACE efficacy with a sensitivity and a specificity of 94.7% and 80%, respectively, when the results were compared with dynamic-CT [27].

MRI is increasingly used in HCC follow-up after TACE. By using dynamic gadolinium-enhanced MR

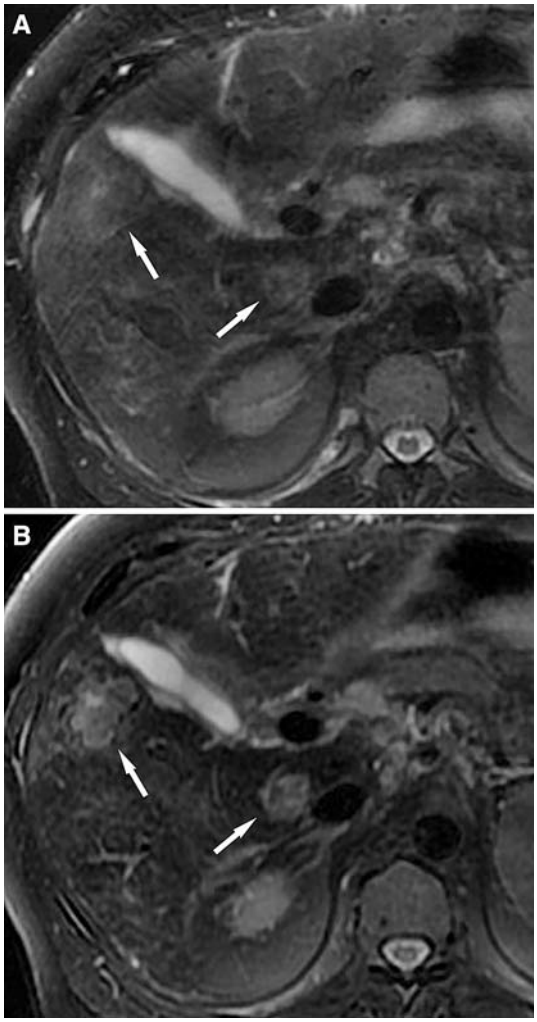


**Fig. 3.** A sixty-year-old male with liver cirrhosis and with two HCC nodules in liver segment 1 and liver segment 5, 30 days after the first TACE session. **A** Transverse respiratory-triggered T2-weighted FSE (7500/87.3 with fat suppression) before SPIO administration. Both nodules are inhomogenous hyperintense compared to the surrounding liver parenchyma (*arrows*). **B** Transverse respiratory-triggered T2-weighted FSE (7500/87.3 with fat suppression) at the same level, 15 min after SPIO administration. Both nodules are clearly seen as marked hyperintense areas compared to the unenhanced images (*arrows*). Both nodules were considered with residual viable tumor and were confirmed at standard of reference.

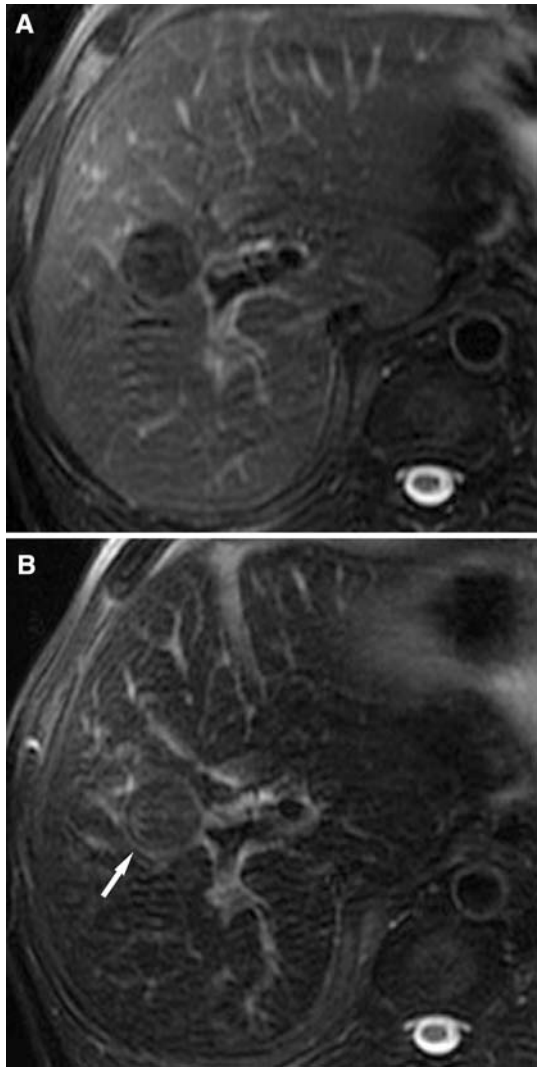


**Fig. 4.** Cirrhotic liver in a 46-year-old male with an HCC nodule in liver segment 5, 30 days after the second TACE session. **A** Transverse respiratory-triggered T2-weighted FSE (6667/99.4 with fat suppression) before SPIO administration. The nodule is well-delineated and homogeneous hypointense compared to the surrounding liver parenchyma. **B** Transverse respiratory-triggered T2-weighted FSE (6667/99.4 with fat suppression) at the same level, 15 min after SPIO administration. The nodule remains homogeneous hypointense without any hyperintense areas. Note the thin pseudocapsule which is hyperintense (*arrow*). The nodule was without viable tumor at standard of reference.

imaging, Murakami et al. [28] were able to accurately assess the TACE efficacy in nine of ten patients using histopathological findings as standard of reference. In another study [29], dynamic gadolinium-enhanced MR imaging showed a sensitivity, specificity and accuracy of 100% for viable tumor detection after TACE. However, in the study of Kubota et al. [29], histological or angiographical correlations were not available in all patients and the authors excluded 14 of 84 nodules (17%). These nodules were considered unsuitable for qualitative assessment of contrast uptake due to the high signal intensity pattern on T1-unenhanced images.

In our study, the double-contrast MR technique was more accurate in viable tumor detection after TACE compared to gadolinium or SPIO techniques alone. With dynamic gadolinium-enhanced technique, we obtained a sensitivity of 68%, a specificity of 100% and an accuracy of 72% for viable tumor detection. Although it was

**Table 3.** Sensitivity, specificity and accuracy for viable tumor detection for each reader and MRI technique

| MR technique | True-positive | | True-negative | | False-positive | | False-negative | | Indeterminate | | Sensitivity | | | Specificity | | | Accuracy | | |
|---|---|---|---|---|---|---|---|---|---|---|---|---|---|---|---|---|---|---|---|
| | R1 (n) | R2 (n) | R1 (n) | R2 (n) | R1 (n) | R2 (n) | R1 (n) | R2 (n) | R1 (n) | R2 (n) | R1 (%) | R2 (%) | Mean (%) | R1 (%) | R2 (%) | Mean (%) | R1 (%) | R2 (%) | Mean (%) |
| Gadolinium-enhanced | 15 | 15 | 3 | 3 | 0 | 0 | 7 | 7 | 5 | 5 | 68 | 68 | 68 | 100 | 100 | 100 | 72 | 72 | 72 |
| SPIO-enhanced | 18 | 20 | 4 | 4 | 0 | 0 | 5 | 4 | 3 | 2 | 78 | 83 | 80 | 100 | 100 | 100 | 81 | 85 | 83 |
| Double-contrast enhanced | 24 | 24 | 4 | 4 | 0 | 0 | 2 | 2 | 0 | 0 | 92 | 92 | 92 | 100 | 100 | 100 | 93 | 93 | 93 |

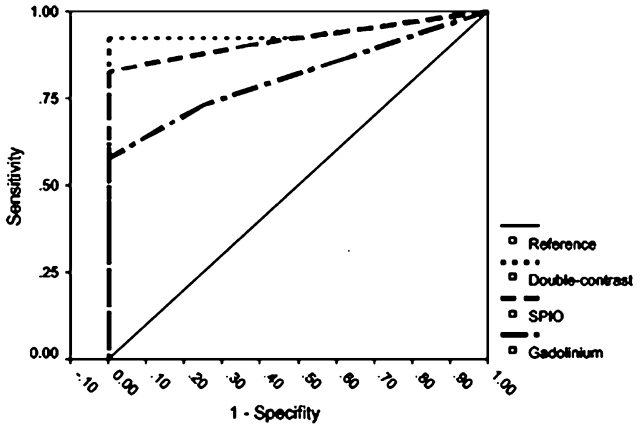


Fig. 5. ROC curves for viable tumor detection with means of both observers for gadolinium-enhanced technique, SPIO-enhanced technique, and double-contrast enhanced technique. Sequential administration of gadolinium and SPIO combined resulted in the best performance for detection of viable tumor after TACE.

reported that iodized oil emulsion produces high signal areas on T1-unenhanced images just over the first few days following TACE [30], 17 of 30 nodules (56%) were homogeneously or inhomogeneously hyperintense on T1-unenhanced images in our study. These lesions were responsible for most of the false negative results. One explanation of the high signal intensity of the nodules after TACE on T1-unenhanced images may be represented by the coagulative necrosis [31, 32]. Our findings are in agreement with the results of other studies in which half of nodules were hyperintense on T1-unenhanced images after TACE [33]. Results of our study indicate that the SPIO-enhanced technique was more sensitive (80%) and accurate (83%) compared to the gadolinium-enhanced technique (68% sensitivity and 72% accuracy) without any statistically significant difference. The diagnosis of viable HCC was based on the signal intensity pattern on T2-weighted images before and after SPIO administration. The rationale for the fact why SPIO-enhanced MR imaging may increase the diagnostic performance for detection of viable tumor might be explained by the following hypothesis. Immediately after TACE, in acute phase of cytotoxicity there are areas of liquefied necrosis which are hyperintense on T2-weighted images [34]. In a later phase, an area that is completely embolized by TACE usually demonstrates low signal intensity on unenhanced T2-weighted MR images (due to coagulative necrosis) [32]. The signal intensity of these areas is unchanged on T2-weighted images after SPIO administration. Hyperintense foci within these hypointense nodules or along its periphery may represent one month after TACE viable tumor on T2-unenhanced images. These hyperintense foci may be barely visible on T2-unenhanced images. Due to the fact that following SPIO administration the signal of the surrounding liver parenchyma decreases, these hyperintense foci are becoming more conspicuous in particular if they are located within the periphery of the nodule. The false negative results were represented by nodules homogeneous hypointense on both T2-weighted images, before and after SPIO administration (2 nodules for reader 1 and one nodule for reader 2). This may be as a result of the fact that small foci of HCC are only visible at histology [3]. Three false negative results were caused by nodules with hyperintense areas on T2-unenhanced images which decreased in signal intensity after SPIO administration. However, it is known that well-differentiated HCs may contain Kupfer cells and show some uptake of SPIO. This lesions can be missed on SPIO technique [35].

In comparison to gadolinium technique and SPIO technique, double-contrast technique was more accurate (92%) in viable tumor detection after TACE. By combining the strong vascular enhancement of gadolinium on one hand and the SPIO's tissue specific information on the other, both readers were able to detect viable tumor in 24 of 26 nodules with viable tumor at standard of reference. In two nodules assessed as nodules without viable tumor, small areas of HCC were found at histology. Both nodules were hyperintense on T1-unenhanced images and displayed a decrease in signal intensity on T2-weighted images after SPIO administration.

We acknowledge the following limitations. We did not compare MR images with any cross-sectional image modality performed prior to TACE. Therefore the size of the treated lesion was not an interpretation criteria. However, it has been demonstrated that the rate of tumor-size reduction does no correlate with the therapeutic effect

of chemoembolization [15]. The time point of follow-up and the interval between double-contrast MR examination and standard of reference can be considered as another limitation. In this study we evaluated the patients with MR imaging 4 weeks after TACE. A one month interval after TACE is necessary in order to avoid mistakes when evaluating areas with nonspecific iodized oil emulsion deposition. In this interval iodized oil gradually washes-out from nonnecrotic areas of HCC and surrounding parenchyma [15]. Regarding the interval between MR studies and final confirmatory results, we considered that the presence of viable HCC within a treated nodule is the result of the progression of residual tumor after TACE and does not indicate a de novo or a remote HCC.

We did not make a quantitative assessment of the signal intensity of the nodules on gadolinium-enhanced images. This might have improved the gadolinium-enhanced technique performance especially for those nodules which were hyperintense on T1-unenhanced images. However, the signal intensity changes by means of region of interest (ROI) measurements should be obtained within suspicious areas of enhancement. Since the exact localization and extent of these areas are difficult to evaluate in nodules which are homogeneous or inhomogeneous hyperintense on T1-unenhanced images, the results of signal intensity measurements highly depend on the location of the ROI. Another potential limitation might be the fact that the enhancement pattern of the extracellular contrast medium could have been influenced by the prior administration of the SPIO. Although, SPIO affects the signal intensity of normal liver parenchyma on both T1- and T2-weighted images , this signal reduction does not influence the gadolinium enhancement and so the analysis of hypervascular areas is not affected [35].

A histopathological analysis was not possible for all nodules and DSA was performed in those cases with suspicion of viable HCC based on serum alfafetoprotein level or double-contrast MR images. In five nodules, the suspicion was based on the areas of hypervascularity on MR images. However, DSA is considered a reliable imaging modality for assessment of viable tumor [6, 7]. Finally, the number of nodules in this study was relatively small, so further studies with a larger number of nodules are needed to reach a firmer conclusion.

In conclusion, this study shows that double-contrast MR technique (i.e., the sequential administration of SPIO and gadopentetate dimeglumine contrast agents) may be a useful strategy for the treatment response evaluation of HCC in cirrhotic liver after TACE. Double-contrast MR technique significantly improves the viable tumor detection in HCC's treated with TACE compared to gadolinium-enhanced and SPIO-enhanced techniques.

## References


1. Bruix J, Llovet JM (2002) Prognostic prediction and treatment strategy in hepatocellular carcinoma. Hepatology 35:519–524
2. Llovet JM, Bru C, Bruix J (1999) Prognosis of hepatocellular carcinoma: the BCLC staging classification. Semin Liver Dis 19:329–338
3. Ito K, Honjo K, Fujita T, et al. (1995) Therapeutic efficacy of transcatheter arterial chemoembolization for hepatocellular carcinoma: MRI and pathology. J Comput Assist Tomogr 19:198–203
4. Ward J, Guthrie JA, Scott DJ, et al. (2000) Hepatocellular carcinoma in the cirrhotic liver: double-contrast MR imaging for diagnosis. Radiology 216:154–162
5. Earls JP, Rofsky NM, DeCorato DR, Krinsky GA, Weinreb JC (1997) Hepatic arterial-phase dynamic gadolinium-enhanced MR imaging: optimization with a test examination and a power injector. Radiology 202:268–273
6. Castrucci M, Sironi S, De Cobelli F, Salvioni M, Del Maschio A (1996) Plain and gadolinium-DTPA-enhanced MR imaging of hepatocellular carcinoma treated with transarterial chemoembolization. Abdom Imaging 21:488–494
7. Yoshioka H, Nakagawa K, Shindou H, et al. (1990) MR imaging of the liver before and after transcatheter hepatic chemo-embolization for hepatocellular carcinoma. Acta Radiol 31:63–67
8. Landis JR, Koch GG (1977) An application of hierarchical kappa-type statistics in the assessment of majority agreement among multiple observers. Biometrics 33:363–374
9. Imaeda T, Yamawaki Y, Seki M, et al. (1993) Lipiodol retention and massive necrosis after lipiodol-chemoembolization of hepatocellular carcinoma: correlation between computed tomography and histopathology. Cardiovasc Intervent Radiol 16:209–213
10. Matsui O, Kadoya M, Yoshikawa J, Gabata T, Takashima T, Demachi H (1994) Subsegmental transcatheter arterial embolization for small hepatocellular carcinomas: local therapeutic effect and 5-year survival rate. Cancer Chemother Pharmacol 33(suppl):S84–S88
11. Choi BI, Kim HC, Han JK, et al. (1992) Therapeutic effect of transcatheter oily chemoembolization therapy for encapsulated nodular hepatocellular carcinoma: CT and pathologic findings. Radiology 182:709–713
12. Kenji J, Hyodo I, Tanimizu M, et al. (1997) Total necrosis of hepatocellular carcinoma with a combination therapy of arterial infusion of chemotherapeutic lipiodol and transcatheter arterial embolization: report of 14 cases. Semin Oncol 24:S6-71–S7680
13. Miller DL, O'Leary TJ, Girton M (1987) Distribution of iodized oil within the liver after hepatic arterial injection. Radiology 162:849–852
14. Takayasu K, Shima Y, Muramatsu Y, et al. (1987) Hepatocellular carcinoma: treatment with intraarterial iodized oil with and without chemotherapeutic agents. Radiology 163:345–351
15. Takayasu K, Arii S, Matsuo N, et al. (2000) Comparison of CT findings with resected specimens after chemoembolization with iodized oil for hepatocellular carcinoma. AJR Am J Roentgenol 175:699–704
16. Okusaka T, Okada S, Ueno H, et al. (2000) Evaluation of the therapeutic effect of transcatheter arterial embolization for hepatocellular carcinoma. Oncology 58:293–299
17. Nishimine K, Uchida H, Matsuo N, et al. (1994) Segmental transarterial chemoembolization with Lipiodol mixed with anticancer drugs for nonresectable hepatocellular carcinoma: follow-up CT and therapeutic results. Cancer Chemother Pharmacol 33(suppl):S60–S68
18. Murakami R, Yoshimatsu S, Yamashita Y, Sagara K, Arakawa A, Takahashi M (1994) Transcatheter hepatic subsegmental arterial chemoembolization therapy using iodized oil for small hepatocellular carcinomas. Correlation between lipiodol accumulation pattern and local recurrence. Acta Radiol 35:576–580
19. Vogl TJ, Trapp M, Schroeder H, et al. (2000) Transarterial chemoembolization for hepatocellular carcinoma: volumetric and morphologic CT criteria for assessment of prognosis and therapeutic success-results from a liver transplantation center. Radiology 214:349–357
20. Minami Y, Kudo M, Kawasaki T, et al. (2003) Transcatheter arterial chemoembolization of hepatocellular carcinoma: usefulness

of coded phase-inversion harmonic sonography. AJR Am J Roentgenol 180:703–708
21. Sze DY, Razavi MK, So SK, Jeffrey RB Jr (2001) Impact of multidetector CT hepatic arteriography on the planning of chemoembolization treatment of hepatocellular carcinoma. AJR Am J Roentgenol 177:1339–1345
22. Koito K, Namieno T, Ichimura T, et al. (2000) Power Doppler sonography: evaluation of hepatocellular carcinoma after treatment with transarterial embolization or percutaneous ethanol injection therapy. AJR Am J Roentgenol 174:337–341
23. Cioni D, Lencioni R, Bartolozzi C (2000) Therapeutic effect of transcatheter arterial chemoembolization on hepatocellular carcinoma: evaluation with contrast-enhanced harmonic power Doppler ultrasound. Eur Radiol 10:1570–1575
24. Sumi S, Yamashita Y, Mitsuzaki K, et al. (1999) Power Doppler sonography assessment of tumor recurrence after chemoembolization therapy for hepatocellular carcinoma. AJR Am J Roentgenol 172:67–71
25. Murakami T, Nakamura H, Hori S, et al. (1993) Detection of viable tumor cells in hepatocellular carcinoma following transcatheter arterial chemoembolization with iodized oil. Pathologic correlation with dynamic turbo-FLASH MR imaging with Gd-DTPA. Acta Radiol 34:399–403
26. Lagalla R, Caruso G, Finazzo M (1998) Monitoring treatment response with color and power Doppler. Eur J Radiol 27(suppl 2):S149–S156
27. Youk JH, Lee JM, Kim CS (2003) Therapeutic response evaluation of malignant hepatic masses treated by interventional procedures with contrast-enhanced agent detection imaging. J Ultrasound Med 22:911–920
28. Murakami T, Nakamura H, Tsuda K, et al. (1993) Treatment of hepatocellular carcinoma by chemoembolization: evaluation with 3DFT MR imaging. AJR Am J Roentgenol 160:295–299
29. Kubota K, Hisa N, Nishikawa T, et al. (2001) Evaluation of hepatocellular carcinoma after treatment with transcatheter arterial chemoembolization: comparison of Lipiodol-CT, power Doppler sonography, and dynamic MRI. Abdom Imaging 26:184–190
30. De Santis M, Alborino S, Tartoni PL, Torricelli P, Casolo A, Romagnoli R (1997) Effects of lipiodol retention on MRI signal intensity from hepatocellular carcinoma and surrounding liver treated by chemoembolization. Eur Radiol 7:10–16
31. Sakurai M, Okamura J, Kuroda C (1984) Transcatheter chemoembolization effective for treating hepatocellular carcinoma. A histopathologic study. Cancer 54:387–392
32. Marukawa T, Harada K, Kuruda C (1987) MRI of the resected hepatocellular carcinoma specimens following trans-catheter arterial embolization. Comparison with pathologic findings (Abstract). In: 5th Asian oceanian congr radiol, vol 47
33. Yan FH, Zhou KR, Cheng JM, et al. (2002) Role and limitation of FMPSPGR dynamic contrast scanning in the follow-up of patients with hepatocellular carcinoma treated by TACE. World J Gastroenterol 8:658–662
34. Ohtomo K, Itai Y, Yoshikawa K, Yashiro N, Kokubo T, Iio M (1986) MR imaging of hepatoma treated by embolization. J Comput Assist Tomogr 10:973–975
35. Noguchi Y, Murakami T, Kim T, et al. (2003) Detection of hepatocellular carcinoma: comparison of dynamic MR imaging with dynamic double arterial phase helical CT. AJR Am J Roentgenol 180:455–460